Edge Momentum Transport by Neutrals

J.T. Omotani[1], S.L. Newton[1,2], I. Pusztai[1] and T. Fülöp[1]

[1]Department of Physics, Chalmers University of Technology, 41296 Gothenburg, Sweden
[2]CCFE, Culham Science Centre, Abingdon, Oxon, OX14 3DB, UK

Corresponding Author: omotani@chalmers.se

Abstract:

Due to their high cross-field mobility, neutrals can contribute to momentum transport even at the low relative densities found inside the separatrix and they can generate intrinsic rotation. We use a charge-exchange dominated solution to the neutral kinetic equation, coupled to neoclassical ions, to evaluate the momentum transport due to neutrals. Numerical solutions to the drift-kinetic equation allow us to model the intermediate collisionality typical of the tokamak edge. In the edge there are several processes likely to contribute to momentum transport in addition to neutrals. Therefore, we present here an interpretative framework that can evaluate the momentum transport through neutrals based on radial plasma profiles. We demonstrate its application with representative artificial profiles and an analytical equilibrium, with parameters typical of L-mode in a medium-sized tokamak. The magnitudes of the torques we find here due to neutrals are 0.5–5 N·m, motivating the application of our framework to experimental data, where it will allow us to evaluate the importance of the momentum flux due to neutrals compared to other transport mechanisms.

1 Introduction

Momentum transport in the tokamak edge is a crucial issue since rotation suppresses magnetohydrodynamic instabilities such as resistive wall modes [1] and flow shear in the edge suppresses turbulence, leading to high-confinement mode (H-mode) operation [2]. Neutral particles are always present in the edge of the confined plasma volume, and despite their low relative density can contribute strongly to transport due to their high cross-field mobility, as has been demonstrated theoretically [3–12]. The influence of neutrals on confinement has also been observed experimentally [13–15] and the poloidal location of gas-fuelling, inboard vs. outboard, has been seen to be important for the low- to high-confinement transition threshold [16–18].

It has been shown previously that when neutrals dominate the angular momentum transport, the radial electric field and hence toroidal rotation can be self-consistently calculated [10–12]. However, there will be other contributions, potentially of similar or greater magnitude, for instance from turbulence, ion orbit losses [19], non-axisymmetric magnetic fields or finite orbit width effects [20]. It is therefore important to evaluate the momentum transport due to neutrals from experimental profiles, so that the magnitudes of the various effects can be compared. Analytical solutions [10, 11] rely on asymptotic ordering of the collisionality into Pfirsch-Schlüter (high collisionality) or banana (low collisionality) regimes. However, the conditions typical in the edge plasma produce order unity collisionality $\nu_{\mathrm{ii}} L_\parallel / v_T \sim 1$, where v_T is the thermal velocity, ν_{ii} the ion-ion collision

rate and $L_\parallel = \oint d\theta \left(dl_\parallel/d\theta\right)/2\pi$ the parallel connection length. In order to relax this constraint numerical solutions of the drift-kinetic equation must be used. Recently, the radial electric field and toroidal rotation have been calculated numerically from the constraint that the momentum flux through neutrals vanishes in steady state [12] that is, as noted above, assuming that the neutrals dominate the momentum transport and also that the radial gradient of the neutrals is the dominant profile gradient. The latter assumption makes the calculation of the momentum flux local (otherwise it would depend on, for instance, the radial gradient of the toroidal rotation and hence on second derivatives of the density, temperature, etc.). Here, in order to avoid these assumptions, we introduce a new approach which takes the background plasma profiles, including the radial electric field, as given and allows us to calculate the momentum flux through neutrals directly, without requiring that they are the only channel for momentum transport. This provides an interpretative tool that can be applied to experimental data in order to compare the magnitude of the neutral momentum transport to other mechanisms and to externally applied torques. The interpretative approach is derived in Section 2 and applied to representative artificial profiles in Section 3; in Section 4 we return to the predictive approach for comparison to the new results.

2 Neutral momentum transport

We outline here the calculation of the momentum flux through neutrals, which are coupled by charge exchange to kinetic ions. Integrated over a flux surface, the flux of toroidal angular momentum carried by the neutral population is $V' \left\langle R\hat{\boldsymbol{\zeta}} \cdot \boldsymbol{\Pi}_\mathrm{n} \cdot \nabla\psi \right\rangle$ where $\boldsymbol{\Pi}_\mathrm{n} = m_\mathrm{i} \int d^3v\, \boldsymbol{vv} f_\mathrm{n}$ is the stress tensor of the neutrals, f_n is the distribution function of the neutrals, ψ is 2π times the poloidal flux, V is the volume enclosed by a flux surface, a prime denotes a derivative with respect to ψ, R is the major radius, $\hat{\boldsymbol{\zeta}} = \nabla\zeta/\left|\nabla\zeta\right|$ with ζ the toroidal angle, and m_i is the mass of the ions or neutrals.

Our solution to the kinetic equation for f_n relies on several approximations. We take a short charge-exchange (CX) mean-free-path (MFP) expansion; although the MFP is not always short compared to profile length scales in the edge, it was found in [9] that the approximation is surprisingly accurate, compared to a full solution allowing arbitrary MFP for a special class of self-similar profiles. We neglect ionization, but this is most important for the determination of the neutral density profile, which we take as an input; ionization affects the momentum transport only by changing the effective collision rate [6]. We use a simplified CX collision operator [4] that allows us to close the neutral kinetic equation in an efficient way [6], as described below. These approximations allow us to avoid the computational expense of Monte Carlo neutral codes, e.g. EIRENE [21], while retaining coupling to the kinetic ion distribution, rather than only a drifting Maxwellian as implemented in [21].

The steady state neutral kinetic equation then takes the form [6]

$$\boldsymbol{v} \cdot \nabla f_\mathrm{n} = \frac{1}{\tau_\mathrm{CX}} \left(\frac{n_\mathrm{n}}{n_\mathrm{i}} f_\mathrm{i} - f_\mathrm{n} \right), \tag{1}$$

where n_n and n_i are the neutral and ion densities and f_i is the ion distribution function. $\tau_\mathrm{CX}^{-1} = n_\mathrm{i} \left\langle \sigma v \right\rangle_\mathrm{CX}$ is the characteristic rate for charge-exchange interactions with $\left\langle \sigma v \right\rangle_\mathrm{CX}$ the thermal charge exchange rate, $\left\langle \sigma v \right\rangle_\mathrm{CX} = 2.82 \times 10^{-14}\,\mathrm{m^3{\cdot}s^{-1}}$ for Deuterium ions and neutrals at 100 eV [22]. Solving perturbatively for small $\tau_\mathrm{CX} v_T/L$, where v_T is the thermal

speed and L is a characteristic length scale of the background profiles,

$$f_{\mathrm{n}}^{(0)} = \frac{n_{\mathrm{n}}}{n_{\mathrm{i}}} f_{\mathrm{i}} \tag{2}$$

$$f_{\mathrm{n}}^{(1)} = -\tau_{\mathrm{CX}} \boldsymbol{v} \cdot \nabla \left(\frac{n_{\mathrm{n}}}{n_{\mathrm{i}}} f_{\mathrm{i}} \right). \tag{3}$$

$f_{\mathrm{n}}^{(0)}$ contributes a term to the momentum flux which is negligible at $\mathcal{O}(\delta)$ [23], being proportional to $\boldsymbol{\Pi}_{\mathrm{i}}$. Thus we need keep only $f_{\mathrm{n}}^{(1)}$ and so

$$\begin{aligned} V' \left\langle R\hat{\boldsymbol{\zeta}} \cdot \boldsymbol{\Pi}_{\mathrm{n}} \cdot \nabla\psi \right\rangle &= -m_{\mathrm{i}} \tau_{\mathrm{CX}} V' \left\langle R \int d^3v \left(\hat{\boldsymbol{\zeta}} \cdot \boldsymbol{v} \right) (\nabla\psi \cdot \boldsymbol{v}) \, \boldsymbol{v} \cdot \nabla \left(\frac{n_{\mathrm{n}}}{n_{\mathrm{i}}} f_{\mathrm{i}} \right) \right\rangle \\ &\approx -m_{\mathrm{i}} \tau_{\mathrm{CX}} \frac{d}{d\psi} \left(V' \left\langle \frac{R n_{\mathrm{n}}}{n_{\mathrm{i}}} \int d^3v \left(\hat{\boldsymbol{\zeta}} \cdot \boldsymbol{v} \right) (\nabla\psi \cdot \boldsymbol{v})^2 f_{\mathrm{i}} \right\rangle \right), \end{aligned} \tag{4}$$

neglecting $\nabla^2\psi$ and using the identities $\langle \nabla \cdot \boldsymbol{A} \rangle = \frac{1}{V'} \frac{d}{d\psi} \left(V' \langle \nabla\psi \cdot \boldsymbol{A} \rangle \right)$ for any $\boldsymbol{A}$ [23] and $\boldsymbol{vv} : \nabla \left(R\hat{\boldsymbol{\zeta}} \right) = 0$[1]. Including the gyroradius correction, the ion distribution function at the particle position $\boldsymbol{r}$ is

$$f_{\mathrm{i}}(\boldsymbol{r}) = f_{\mathrm{i,gc0}}(\boldsymbol{r}) - \frac{e\Phi_1}{T_{\mathrm{i}}} f_{\mathrm{i,gc0}}(\boldsymbol{r}) - \boldsymbol{\rho} \cdot \nabla f_{\mathrm{i,gc0}}(\boldsymbol{r}) + g_{\mathrm{i}}(\boldsymbol{r}) \tag{5}$$

where $f_{\mathrm{i,gc0}}$ is a Maxwellian, $\boldsymbol{\rho} = \boldsymbol{r} - \boldsymbol{R}_{\mathrm{gc}}$ is the gyroradius vector with $\boldsymbol{R}_{\mathrm{gc}}$ the guiding centre position, $\Phi_1 = \Phi - \langle \Phi \rangle$ is the poloidally varying part of the electrostatic potential Φ and 0, 1 subscripts refer to the order in a $\delta = \rho/L$ gyroradius expansion. The first two terms do not contribute to (4) as they are isotropic in $\boldsymbol{v}$. We obtain the non-adiabatic piece of the perturbed distribution function, $g_{\mathrm{i}} = f_{\mathrm{i},gc1} + e_{\mathrm{i}}\Phi_1 f_{\mathrm{i,gc0}}/T_{\mathrm{i}}$ from numerical solutions of the first order drift kinetic equation using the PERFECT neoclassical solver (run here in radially-local mode) [24], which assume that the flow is subsonic, $\boldsymbol{V} \sim \mathcal{O}(\delta v_T)$.

3 Neutral contribution

In order to gain insight into the potential importance of the neutrals for rotation in the edge in the presence of NBI torque and for comparison to other momentum transport mechanisms, we evaluate the neutral momentum flux (4) for representative background profiles with parameters typical of a medium-sized tokamak. For the equilibrium we take analytical solutions to the Grad-Shafranov equation [25][2]. The input parameters of the equilibrium are characteristic of ASDEX Upgrade: major radius of the plasma centre $R_0 = 1.65\,\mathrm{m}$, inverse aspect ratio $\epsilon = 0.303$, elongation $\kappa = 1.8$, triangularity $\delta = 0.2$, vacuum magnetic field at the plasma centre $B_0 = -2.5\,\mathrm{T}$, normalized toroidal pressure $\beta_{\mathrm{T}} = 0.03$ and plasma current $I_{\mathrm{p}} = 800\,\mathrm{kA}$. The assumed background profiles used throughout this section and the next are shown in FIG. 1. We consider neutrals with poloidal profiles that are uniform, Gaussian (with width $\pi/5\,\mathrm{rad}$) or δ-function, keeping the flux-surface averaged density profile $\langle n_{\mathrm{n}} \rangle = 10^{17} \exp\left(-(1-\rho_{\mathrm{pol}})/0.03\right)\ \mathrm{m}^{-3}$ fixed, where $\rho_{\mathrm{pol}} = \sqrt{\psi/\psi_{\mathrm{sep}}}$ is a flux coordinate with ψ_{sep} the value of ψ at the separatrix. The maximum local density for the Gaussian profile reaches $1.3 \times 10^{18}\,\mathrm{m}^{-3}$ at $\rho_{\mathrm{pol}} = 0.995$.

[1] This identity follows from the fact that $\boldsymbol{vv}$ is a symmetric tensor, while $\nabla \left(R\hat{\boldsymbol{\zeta}} \right)$ is antisymmetric.

[2] Evaluated in Python using an implementation available at [26]

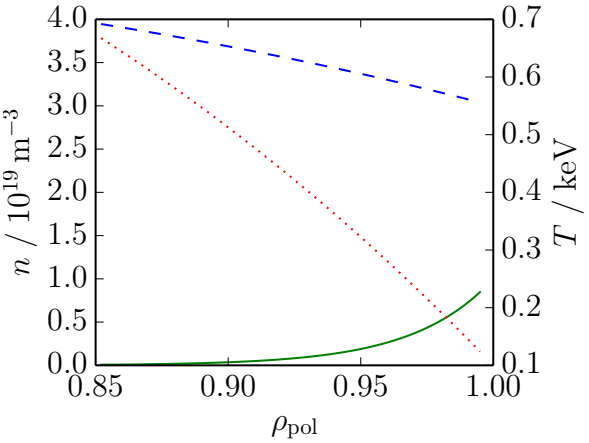

FIG. 1: Profiles used for the simulation as a function of ρ_{pol}: ion density n_{i} (blue, dashed); flux surface average of the neutral density $\langle n_{\mathrm{n}} \rangle \times 100$ (green, solid); and ion temperature T_{i} (red, dotted).

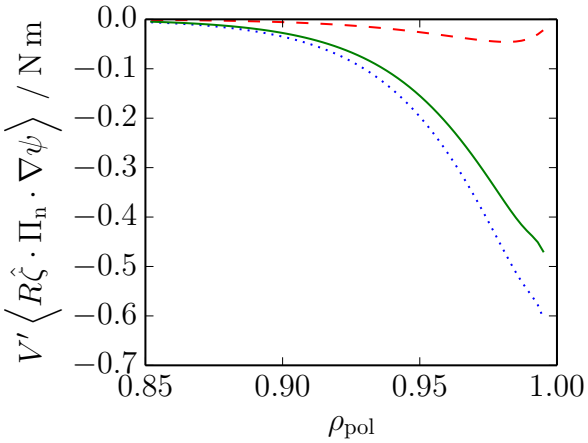

FIG. 2: Momentum flux through neutrals as a function of ρ_{pol}. Poloidal profiles are δ-function at outboard midplane (blue, dotted), Gaussian with width $\pi/5$ rad centred at outboard midplane (green, solid) and uniform (red, dashed).

This is broadly consistent with modelling of ASDEX discharges with outboard gas-puff [27].

The neutrals provide more effective transport of toroidal angular momentum when they are on the outboard side of the tokamak, due to the larger major radius and poloidal magnetic field B_{p}, as can be seen from (4), noting that $|\nabla\psi| = RB_{\mathrm{p}}$. The poloidal distribution of the neutrals is therefore expected to be important. FIG. 2 shows the momentum transport in the absence of a radial electric field; we can see that the difference in momentum flux between the cases with uniformly distributed and outboard localized neutrals is large. Previous work, both analytical [10, 11] and numerical [12], used δ-function localized neutrals for convenience. We can also see from FIG. 2 that there is only a small difference between this approximation and the case of neutrals localized near the outboard midplane as a Gaussian.

When the neutrals are localized on the outboard side of the plasma, the momentum flux for the model case considered approaches $-0.5\,\mathrm{N{\cdot}m}$. For comparison 1 MW of NBI heating at R_0 with 100 keV particles gives 1.1 N·m of torque. This indicates the significance of the momentum flux through neutrals, especially when modelling intrinsic rotation and for the sustainment of an edge transport barrier.

We now consider the effect of the radial electric field E_r. Strong fields appear in H-mode in the edge transport barrier, and the orderings of neoclassical theory begin to break down, but even in L-mode there can be a well in the radial electric field at the edge [28]. The radial electric field E_r enters f_{i} only through the toroidal velocity, since we assume a low flow ordering $V \sim \delta\, v_T$ here. The momentum flux driven through neutrals by ∇E_r is therefore

$$\left| V' \left\langle R\hat{\boldsymbol{\zeta}} \cdot \boldsymbol{\Pi}_{\mathrm{n}} \cdot \nabla\psi \right\rangle \right|_{\nabla E_r} = -\tau_{\mathrm{CX}} V' \left\langle R^2 T_{\mathrm{i}} n_{\mathrm{n}} \frac{dE_r}{dr} \right\rangle$$

$$\approx -0.24\,\mathrm{N\,m} \left[n_{\mathrm{i}} / 3 \times 10^{19}\,\mathrm{m}^{-3} \right]^{-1} \left[T_{\mathrm{i}} / 100\,\mathrm{eV} \right]^{\frac{1}{2}} \left[\langle n_{\mathrm{n}} \rangle / 10^{17}\,\mathrm{m}^{-3} \right] \left[\frac{dE_r}{dr} / \mathrm{kV{\cdot}m^{-2}} \right] \quad (6)$$

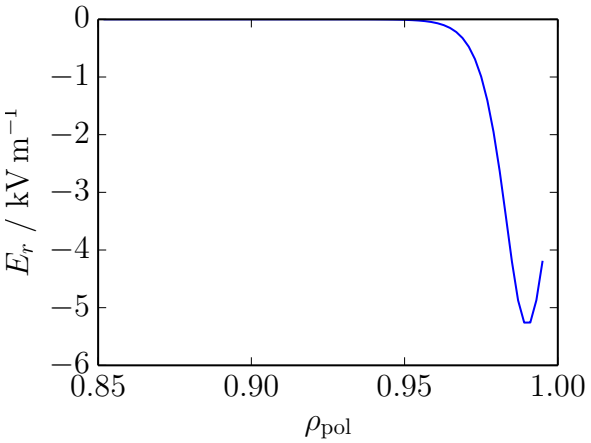

FIG. 3: Radial electric field E_r at the outboard midplane as a function of ρ_{pol}.

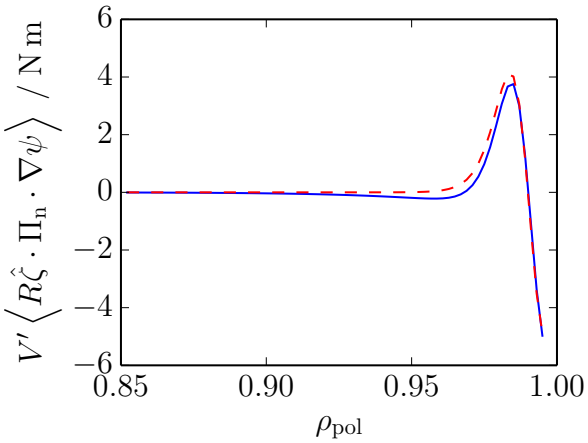

FIG. 4: Momentum flux through neutrals as a function of ρ_{pol}—full flux (4) (blue, solid) and approximate dE_r/dr piece (6) (red, dashed)—for E_r shown in FIG. 3 with neutrals localized as a δ-function at the outboard midplane.

where the last line is evaluated for neutrals localized as a δ-function at the outboard midplane and with the separatrix parameters $R = 2.15\,\mathrm{m}$ and $V'(\rho_{\mathrm{pol}} = 0.995) \approx 27.4\,\mathrm{T}^{-1}\cdot\mathrm{m}$.

To show the magnitude of the momentum flux driven by E_r shear, we take the E_r well shown in FIG. 3 as an input, which is of the size observed in experiment [28]. The gradient length scale of the electrostatic potential is $L_\Phi = T_{\mathrm{i}}/eE_r \gtrsim 2\,\mathrm{cm}$ while the poloidal gyroradius is smaller $\sqrt{2m_{\mathrm{i}}T_{\mathrm{i}}}/eB_{\mathrm{p}} \approx 0.5\,\mathrm{cm}$, so the local drift-kinetic ordering is satisfied for this E_r well. FIG. 4 compares the full momentum flux (4) and the piece driven by dE_r/dr (6), showing that for these background profiles the electric field shear drive dominates the momentum flux through neutrals. The size of the momentum flux in the E_r well is comparable to the NBI torque (for outboard localized neutrals) indicating their importance for edge momentum transport.

4 Neutral dominated rotation

In order to see whether the neutrals alone can generate an E_r comparable to that seen in L-mode experiments, in this section we return to the procedure presented in [12] to evaluate the self-consistent edge electric field for which the momentum flux vanishes, when neutrals dominate the momentum transport. Note that in this section we assume, as discussed above and in [12], that other background gradients can be neglected compared to $dn_{\mathrm{n}}/d\psi$ when evaluating (4). We must pick a flux surface for this method; we use the $\rho_{\mathrm{pol}} = 0.975$ surface, which is near enough to the plasma edge to still have a substantial neutral density. The temperature, density and their gradients are taken from the profiles in FIG. 1. A scan in the poloidal location of the neutrals, showing the effect of changing the gas fuelling location, is shown as the green, solid curve in FIG. 5. We also plot, as dashed curves, scans for higher and lower bulk ion collisionalities where the density is varied with fixed logarithmic gradients; this scan demonstrates that, as expected from the value of the collisionality $\nu_{\mathrm{ii}}L_\parallel/v_T = 0.532$, the ions are intermediate between the asymptotically high and low collisionality regimes where, as shown in [29], the simulation values

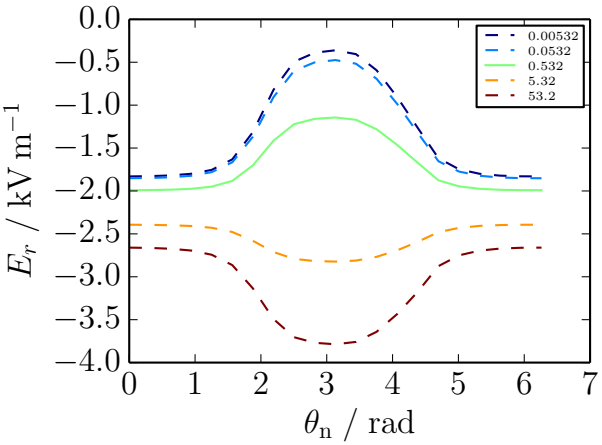

FIG. 5: Radial electric field E_r as a function of poloidal location of the neutrals θ_n. Legend shows collisionality of passing particles. Solid line is nominal collisionality.

approach the analytical limits. The values of the electric field generated purely by the neutral effect considered here, FIG. 5, are smaller but of similar magnitude to those examined in FIGs. 3 and 4, which are relevant to experimental L-mode observations [28]. Since in these solutions the output electric field is proportional to the input temperature gradient, for stronger intrinsic rotation to be driven by neutrals, strong temperature gradients are required; these are challenging for standard neoclassical (or gyrokinetic) transport modelling since they drive the order zero distribution function away from Maxwellian. Despite the challenges, progress is being made in neoclassical pedestal modelling [24, 30–32].

5 Discussion

We have demonstrated that charge-exchanging neutrals can carry a significant momentum flux in the tokamak edge, potentially comparable to the NBI torque if the neutrals are localized on the outboard side of the plasma. The formalism developed in [10, 11] and first implemented numerically in [12] has been extended to enable interpretative studies evaluating the momentum transport through neutrals for experimental profiles and equilibria. In this interpretative mode, the radial variation of the background profiles does not have to be neglected compared to the radial gradient of the neutral density. We use inputs characteristic of an L-mode plasma in a medium sized tokamak to demonstrate this capability and show that a significant flux of momentum can be carried by the neutrals, motivating the application to experimental data in future.

The approach taken here allows rapid experimentation with parameters and profiles and provides both qualitative insight and at least order of magnitude estimates of the momentum transport due to neutrals. Despite the limitations of the modelling described here, some qualitative conclusions are clear. The strength of the neutral momentum transport is much stronger for neutrals located on the outboard side of the tokamak than on the inboard side. This is due both to the smaller moment of force due to smaller major radius and to the smaller physical-space gradients of flux-function plasma profiles which have poloidally constant gradients in ψ-space, as $|\nabla\psi| = RB_p$ is smaller on the inboard side. Likewise near the X-point, where B_p is small, the influence of the neutrals will be weak. Therefore the braking of externally driven rotation will be larger (more unfavourable) for outboard than inboard or X-point neutrals, favouring fuelling from the inboard side or X-point. On the other hand, if it is desired to drive intrinsic rotation using the neutral momentum flux, then this will compete more effectively with other momentum transport channels if the neutrals are located on the outboard side and might be able to generate substantial radial electric fields in H-mode pedestals.

Intrinsic rotation is particularly important for future tokamaks such as ITER since the torque from NBI heating will be weaker in larger devices. The interesting case, as we have seen, is with steep temperature profiles in H-mode, but modelling these is ex-

tremely challenging since the deviations from a Maxwellian distribution are not small, so that a non-linear collision operator is needed, and the steep gradients also necessitate radially-global solutions. State of the art numerical solutions of the neutral kinetic equation couple only to a drifting-Maxwellian plasma [21]. However, the temperature gradient driven departure of the ions from a local Maxwellian distribution drives a momentum flux in the neutral distribution function [4, 11]. Thus when the external torque is large, so that the rotation driven momentum flux dominates, the drifting-Maxwellian description of the plasma is sufficient, but when there are steep temperature gradients, or for intrinsic rotation where the external torque vanishes, a kinetic model for the plasma is needed. In the linear region where standard neoclassical theory and modelling are valid, the transport is proportional to the gradients, so significantly stronger momentum transport through neutrals may be expected in steep gradient regions, such as the H-mode pedestal, although quantitative evaluation, requiring the development of more sophisticated codes coupling fully kinetic neutrals to kinetic ions, remains a challenging subject for future research.

Acknowledgements

The authors are grateful to Matt Landreman for advice and help with the PERFECT code and to Stuart Henderson for assistance with the ADAS database. This work was supported by the Framework grant for Strategic Energy Research (Dnr. 2014-5392) and the International Career Grant (Dnr. 330-2014-6313) from Vetenskapsrådet.

References

[1] HENDER, T. et al., Nucl. Fusion **47** (2007) S128.

[2] TERRY, P. W., Rev. Mod. Phys. **72** (2000) 109.

[3] HAZELTINE, R. et al., Nucl. Fusion **32** (1992) 3.

[4] CATTO, P. J., Phys. Plasmas **1** (1994) 1936.

[5] HELANDER, P. et al., Phys. Plasmas **1** (1994) 3174.

[6] CATTO, P. J. et al., Phys. Plasmas **5** (1998) 3961.

[7] FÜLÖP, T. et al., Phys. Plasmas **5** (1998) 3398.

[8] FÜLÖP, T. et al., Phys. Plasmas **5** (1998) 3969.

[9] FÜLÖP, T. et al., Phys. Plasmas **8** (2001) 5214.

[10] FÜLÖP, T. et al., Phys. Rev. Lett. **89** (2002) 225003.

[11] HELANDER, P. et al., Phys. Plasmas **10** (2003) 4396.

[12] OMOTANI, J. et al., Nuclear Fusion **56** (2016) 124002.

[13] VERSLOOT, T. W. et al., Plasma Phys. Controlled Fusion **53** (2011) 065017.

[14] JOFFRIN, E. et al., Impact of divertor geometry on ITER scenarios performance in the JET metallic wall, in *25th IAEA Fusion Energy Conference*, 2014, EX/P5-40.

[15] TAMAIN, P. et al., J. Nucl. Mater. **463** (2015) 450.

[16] FUKUDA, T. et al., Plasma Phys. Controlled Fusion **42** (2000) A289.

[17] VALOVIC, M. et al., Plasma Phys. Controlled Fusion **44** (2002) A175.

[18] FIELD, A. R. et al., Plasma Phys. Controlled Fusion **46** (2004) 981.

[19] STOLTZFUS-DUECK, T., Phys. Plasmas **19** (2012).

[20] PUSZTAI, I. et al., Plasma Phys. Control. Fusion **58** (2016) 085001.

[21] REITER, D. et al., Fusion Sci. Technol. **47** (2005) 172.

[22] SUMMERS, H. P., *The ADAS User Manual, v. 2.6*, http://www.adas.ac.uk, 2004.

[23] HELANDER, P. et al., *Collisional transport in magnetized plasmas*, Cambridge University Press, 2002.

[24] LANDREMAN, M. et al., Plasma Phys. Controlled Fusion **56** (2014) 045005.

[25] CERFON, A. J. et al., Phys. Plasmas **17** (2010) 032502.

[26] http://github.com/johnomotani/CerfonFreidbergGeometry.

[27] ZHANG, W. et al., Nucl. Fusion **56** (2016) 036007.

[28] VIEZZER, E. et al., Nucl. Fusion **53** (2013) 053005.

[29] OMOTANI, J. T. et al., J. Phys. Conf. Ser. (2016) in press.

[30] CATTO, P. J. et al., Plasma Phys. Control. Fusion **55** (2013) 045009.

[31] BATTAGLIA, D. J. et al., Phys. Plasmas **21** (2014) 072508.

[32] DORF, M. A. et al., Phys. Plasmas **23** (2016) 056102.